Thermodynamic performance of new thermofluidic feed pumps for Organic Rankine Cycle applications

E.S. Richardson

Faculty of Engineering and the Environment,
University of Southampton,
Southampton, SO17 1BJ, UK.
+44 2380594897
e.s.richardson@soton.ac.uk

Abstract

This study develops thermofluidic pump technology that is powered by heat, rather than by electrical or mechanical power. The objective is to improve the performance of heat-recovery by Organic Rankine Cycles, by using a recently-proposed thermofluidic pump. The thermofluidic pump promises low-cost, high-reliability, and, since it does not consume any of the power produced by the expander, improved return on investment. No performance data for the new thermofluidic pump have been reported previously, therefore a thermodynamic model is derived and used to evaluate performance metrics that characterise pump operation and its impact on the overall cycle efficiency. Improved pump configurations are then developed and analysed. A two-stage pump configuration is presented that enhances the thermal efficiency of the cycle. An economiser is also proposed in order to obtain boiler efficiencies similar to those for mechanical feed pumps. It has been shown that the cycle efficiency with the two-stage pump is maximum when there is no net heat input in the intermediate evaporator. The resulting thermal efficiency exceeds the best-possible efficiency that is obtainable with an *ideal* mechanical pump. The relative improvement in cycle efficiency achieved with the two-stage thermofluidic pump is greatest for low-temperature cycles operating below 100°C, for which the back work ratio is usually higher and the efficiencies of electro-mechanical feed pumps are poorer – yielding a relative increase of the cycle efficiency by up to 30%.

Keywords

Organic Rankine Cycle
Feed pump
Thermofluidic
Heat engine
Heat-recovery
Pumpless Rankine Cycle

Nomenclature

Symbols

h	Specific enthalpy
i_{cr}	Specific flow-exergy destroyed due to internal irreversibility
$\dot{m}$	Mass flow rate
p	Pressure
q	Specific heat transferred
s	Specific entropy
T	Temperature
ΔT_{super}	Amount of superheat
ΔT_{pinch}	Pinch point temperature difference
w_x	Specific shaft work transferred
x_q	Specific flow-exergy transferred due to heating.
Y	Volume fraction of liquid

Greek letters

η	Efficiency
ρ	Density
Ψ	Specific flow-exergy

Subscripts

c	Condenser
ev	Evaporator
ex	Exhaust
exp	Expander
s	Denotes isentropic efficiency
pump	Thermodynamic system containing pump
cycle	Thermodynamic system containing the cycle
oa	Overall thermodynamic system including boiler
boiler	Thermodynamic system containing the boiler
in	Input of heat or work
out	Output of heat or work
I	First Law quantity
II	Second Law quantity
0	Dead state conditions (25°C, 1atm)
l	Liquid state
v	Vapour state

Abbreviations

ORC	Organic Rankine Cycle
TFE	Thermal-Fluid Exchange pump
CV	Controlled valve
NRV	Non-return valve

1. Introduction

Rankine-cycle power systems require a feed pump to compress the working fluid. In modern steam cycles within large combustion power plant, the fraction of the expander power consumed by the feed pump, called the back work ratio, is typically only 1% to 3%. Organic Rankine Cycles (ORCs) have been developed in order to make use of lower-temperature heat sources, including geothermal, solar, bio-fuel and surplus process heat [1]. The back work ratio in low-temperature ORCs may be of the order of 10%, making the overall cycle performance increasingly sensitive to the feed pump performance [2].

Mechanical feed pumps are a well-established technology for steam power plant. A review by Quoilin et al. [2] highlights the limited amount of data published for ORC feed pump performance, and reports overall efficiencies (equal to the product of the electrical, mechanical and isentropic efficiencies) for electro-mechanical pumps suitable for kW-scale ORC applications in the range 15-25% [2,3,4,5], whereas Trapp and Colonna [6] propose a value of 65% in the context of a 3MW ORC system based on manufacturer data. Additional requirements of tightness (avoidance of leakage) and reliability are discussed in Ref. [2]. Tightness is important in ORCs due to the cost of the working fluid, and due to safety and environmental considerations affecting some working fluids. Sealing and lubricating mechanical pumps represents a particular challenge. ORC working fluids typically have low lubricity and they may not inhibit corrosion adequately, limiting service life. Because of the relatively high capital costs, the low efficiencies, and the sealing and lubrication challenges associated with mechanical pumps, this study considers thermofluidic feed pumps as an alternative technology for ORCs.

A thermofluidic pump pressurises fluid by thermal expansion, rather than by applying mechanical work. Steam-driven thermofluidic pumps have a long history [7,8], however these thermofluidic pumps have been largely been superseded by mechanical pumps. But the simplicity and low-capital cost of thermo-fluidic pump technology has motivated recent development of pumps employing an organic working fluid and utilising low-temperature solar-thermal energy in order to pump water [9,10]. Yamada et al. [11] recently claimed the first experimental demonstration of a “pumpless” ORC that pressurizes the working fluid thermofluidically, by periodically switching valves and applying unsteady heating to the working fluid in a rigid volume. The back work ratio in a low-temperature ORC with a mechanically-driven feed pump is of the order of 10% [2], requiring that the ORC expander is specified to produce 10% more power than the net power output of the cycle. Because the back work ratio for an ORC with a thermofluidic pump is necessarily zero, use of thermofluidic pumping reduces the required capacity and therefore the cost of the expander. Additional benefits of a thermofluidic pump include long service life and good tightness due to the lack of moving parts.

The Thermal Fluid Exchange (TFE) pump is a thermofluidic device that has been proposed in Ref. [12] as a feed pump for ORCs. A basic implementation of the TFE pump is shown schematically in Fig. **1**. The TFE pump system consists of a condenser, a mass exchange chamber and an evaporator, elevated one above the other as in Fig. **1**. The pump’s condenser and evaporator may be part of the main condenser and evaporator in the ORC, however they are analysed separately in this study for clarity.

The pump operates in a cyclic manner described in Table 1 with the result that low-pressure (p_c) saturated liquid flows into the pump’s condenser and high-pressure (p_{ev}) saturated liquid is discharged from the pump’s evaporator periodically. Figure **1** shows the pump’s components

connected by two non-return valves (NRV1, NRV2) and two controlled valves (CV1, CV2). The valves CV1 and CV2 are controlled in order to achieve a specified volume fraction of liquid in State 1 and another greater volume fraction of liquid in State 3. No performance data for the TFE pump have been reported previously. The objective of this study is therefore to evaluate and improve the thermodynamic performance of the TFE pump, operating within an ORC. Relevant performance metrics and a thermodynamic model for the TFE pump are formulated in Section 2. In Section 3, three additional pump configurations are proposed and their performance is investigated in the context of a simple ORC.

2. Thermodynamic analysis

Mechanical pump performance is characterised conventionally in terms of the mechanical work input using the isentropic efficiency. The TFE pump, in contrast, has no mechanical work input and instead depends on a heat input. Therefore alternative performance metrics are presented for thermofluidic feed pumps in terms of heat inputs (a First Law pump efficiency) and in terms of *exergy* inputs (a Second Law pump efficiency).

The cyclic operation of the TFE pump leads to a periodic fluctuation in the upstream and downstream pressure. The pressure fluctuations can be minimised by a number of practical measures (for example employing more than one pump in parallel with different phasing [12], by use of accumulators, or by flow regulation through CV1 and CV2), therefore periodic fluctuations of condenser and evaporator pressures are neglected in the subsequent analysis. Changes in kinetic energy and gravitational potential energy are negligible compared to changes in the thermal energy in the ORC, and they are also neglected in this analysis.

Heat transfer between the working fluid and the structure of the pump is neglected in the analysis and this is the main limitation of the current modelling. Heat loss to the environment is expected to have a negative impact on the thermal efficiency of the pump, therefore this heat transfer should be minimised through design of the pump (for example by minimising the ratio of surface area to fluid mass and by employing thermal insulation). The analysis below represents the limiting case where the external heat transfer is reduced to zero. Heat transfer between the vapour and liquid within the mass exchange chamber may be significant, depending on the exact implementation of the pump, however, as explained below, the extent of heat transfer between the liquid and vapour does not affect the thermal efficiency of the pump. Therefore, a well-insulated thermal fluid exchange pump with free-flowing valves is expected to approach very closely the predicted thermal efficiencies.

The frequency of the pump operation is expected to be limited by the rate of buoyancy-driven flow through the non-return valves and considering these rate-limiting processes, an estimate for the minimum cycle time is derived in the Appendix. The mass flow rate through the pump is principally affected by the discharge coefficients and flow areas through the non-return valves, and the head of liquid above the respective valves. In combination with the thermodynamic analysis below, the estimated flow rates form a basis on which to specify system components and to conduct preliminary techno-economic optimisation for particular applications.

2.1 Efficiency metrics

The pump is analysed by defining a thermodynamic system comprising a section of the ORC that receives saturated liquid at condenser pressure p_c and delivers saturated liquid at evaporator pressure p_{ev}. The pump analysis system for an ORC with a mechanical pump therefore includes the pump followed by an *economiser* that heats the working fluid up to the saturated liquid state. Assuming that the shaft work input for a mechanical pump is provided by the ORC itself, operating

with First Law cycle efficiency $\eta_{I,cycle}$, an effective specific heat input for the pump analysis system is be defined as

$$q_{in,pump,eff} = q_{in,pump} + w_{x,in,pump}/\eta_{I,cycle} \quad (1)$$

where $q_{in,pump}$ is the actual specific heat input to the pump system and $w_{x,in,pump}$ is the specific shaft work input to the pump. The First Law efficiency of the pump analysis system is then defined as:

$$\eta_{I,pump} = \frac{\left(h_{pump,out} - h_{pump,in}\right)}{q_{eff}}. \quad (2)$$

In steady-state operation the specific enthalpies at pump inlet ($h_{pump,in}$) and outlet ($h_{pump,out}$) are equal to the specific enthalpy of saturated liquid in the condenser ($h_{l,c}$) and evaporator ($h_{l,ev}$) respectively.

The specific flow-exergy is $\psi = (h - h_0) - T_0(s - s_0)$, where s is specific entropy, T is temperature, and subscript '0' refers to the *dead-state*, taken as 25°C and 1atm. The balance equation for ψ is written for one pump cycle as [13],

$$w_{x,in,pump} + x_{q,in,pump} - x_{q,out,pump} - i_{cr,pump} = \psi_{pump,out} - \psi_{pump,in}. \quad (3)$$

Exergy inputs and outputs due to heat addition and rejection respectively are,

$$x_{q,in} = \int \frac{T - T_0}{T} dq_{in}, \text{ and } x_{q,out} = \int \frac{T - T_0}{T} dq_{out}, \quad (4)$$

and i_{cr} is the exergy destroyed by internal irreversibilities. The Second Law component efficiency [14] for the pump analysis system is given by the exergy increase of the fluid divided by the exergy inputs.

$$\eta_{II,pump} = \frac{\psi_{l,ev} - \psi_{l,c}}{w_{x,in,pump} + x_{q,in,pump}}. \quad (5)$$

The First Law cycle efficiency of an ORC is given by the net specific shaft work output divided by the total heat input:

$$\eta_{I,cycle} = \frac{w_{x,out,exp} - w_{x,in,pump}}{q_{in,pump} + q_{in,boiler}}, \quad (6)$$

where $w_{x,out,exp}$ is the expander specific work output. $q_{in,pump}$ is the specific heat input to the pump and $q_{in,boiler}$ is the specific heat input in the remainder of the boiler.

The working fluid in the ORC generally receives heat from a flow of another hotter fluid, described as an exhaust stream in this study. The overall efficiency $\eta_{I,oa}$ describes the fraction of the exhaust stream's sensible heat (relative to the dead state) that is converted into power output, and the boiler efficiency $\eta_{I,boiler}$ is the fraction of the exhaust stream's sensible heat that is transferred into the ORC working fluid:

$$\eta_{I,boiler} = \frac{\dot{m}_{exp}}{\dot{m}_{ex}} \frac{q_{in,pump} + q_{in,boiler}}{h_{ex,in} - h_{ex,0}}, \quad (7)$$

where $h_{ex,0}$ is the enthalpy of the exhaust fluid in the dead state, $T_0 = 25°C$, and $\dot{m}_{exp}/\dot{m}_{ex}$ is the ratio of the cycle-averaged mass flow rates in the expander and in the exhaust. The overall efficiency is given by,

$$\eta_{I,oa} = \eta_{I,boiler}\eta_{I,cycle}. \quad (8)$$

The amount of heat that can be extracted from the exhaust may be subject to practical constraints, depending on the ORC installation. For example, the minimum exhaust temperature may be set in order to provide sufficient buoyancy for satisfactory dispersion of the exhaust plume. In other installations where the ORC draws heat from a closed-loop flow of heat exchange fluid, the temperature change of the heat exchange fluid in the boiler may be limited by the total quantity of heat available, independent of the ORC design. These practical constraints place an upper bound on the boiler efficiency achievable so that the First Law cycle efficiency becomes the prime determinant of the overall efficiency. In this study we impose no constraints on the exhaust exit temperature in order to illustrate the effect of the pump design on the maximum possible value for overall efficiency.

2.2 Modelling assumptions

A thermodynamic model has been derived for a sub-critical un-recuperated ORC shown in Fig. 2 that incorporates:

- An isobaric boiler at pressure p_{ev} that accepts saturated liquid from the feed pump system and delivers vapour to the expander with ΔT_{super} superheat.
- An adiabatic expander with isentropic efficiency $\eta_{s,exp}$.
- An isobaric condenser that accepts fluid from the expander at pressure p_c and delivers saturated liquid to the feed pump system.
- A feed pump system containing either a TFE pump, or a mechanical feed pump followed by an economiser.

Several assumptions are introduced in order to model the TFE feed pump system. The pump is analysed for the limiting case where the mass exchange chamber is completely full of vapour in state 1 and completely full of liquid in state 3. A lumped modelling approach has been adopted for the mass-exchange chamber, assuming that: all of the vapour has one temperature; all of the liquid has another temperature; and the pressure is equal for both phases. Since states 1 and 3 are fixed, the total evaporator heat input and hence the predicted First Law efficiency is independent of any particular assumption concerning the heat exchanged between the liquid and vapour within the mass exchange chamber during the intervening processes. However it is necessary to apply some assumption to the liquid-vapour heat exchange in order to evaluate the pump's Second Law efficiency because the amount of heat exchanged affects the net exergy flux between the mass exchange chamber and the evaporator. The rate of heat transfer between the liquid and vapour depends on the design of the mass-exchange chamber, and one limiting case is considered in this analysis: it is assumed that the heat transferred between phases is negligible during processes 4→1, 1→2, and 2→3 because the liquid-vapour interface is expected to be unperturbed during vapour release (1→2), during gravity-driven emptying (4→1) and during filling (2→3), providing minimal area for heat transfer. It is also assumed that the vapour injection process (3→4) leads to efficient stirring of the mass-exchange chamber and brings the liquid and vapour phases in State 4 into

thermal equilibrium (if more than one phase is present). Heat transfer with the walls of the mass exchange chamber and within the valves are also neglected. The pressure drop through the non-return valves NRV1 and NRV2 are assumed to be zero once open. This simple modelling approach enables derivation of a set of equations describing the performance of the TFE pump concept.

2.3 Cycle calculation

The thermodynamic properties required for the calculations in this study were evaluated using equations of state [15,16,17,18,19] implemented in REFPROP® software [20].

The assumption that liquid enters the mass exchange chamber without transferring heat implies that State 3 consists entirely of saturated liquid at pressure p_c. The density in State 3, ρ_3, therefore equals the density of liquid in the condenser, $\rho_{l,c}$. State 4 is achieved by admitting an isenthalpic flow of vapour from the evaporator until the pressure equals p_{ev}. The mass transferred per unit volume during process 3 → 4 is equal to $\rho_4 - \rho_3$, and the corresponding quantity of internal energy received by the mass exchange chamber is $(\rho_4 - \rho_3)h_{v,ev}$, where $h_{v,ev}$ is the specific enthalpy of vapour in the evaporator. Thermodynamic properties in State 4 can be determined by considering conservation of energy during process 3 → 4 and numerically solving the relation

$$\rho_4 u_4 = \rho_3 u_3 + (\rho_4 - \rho_3)h_{v,ev}, \tag{9}$$

subject to the constraint that the pressure equals p_{ev}. It is observed that State 4 corresponds to sub-cooled liquid for all calculations presented in this study. In process 4 → 1, vapour from the evaporator completely displaces all liquid from the mass exchange chamber without exchanging heat, therefore State 1 consists entirely of dry-saturated vapour at pressure p_{ev}. The resulting mass exchange chamber states 1 to 4 are shown in Fig. 2, indicating that the pump processes resemble the Rankine cycle in state space.

During steady-state operation, the heat input to the TFE pump can be determined by writing an energy balance for the pump's evaporator during one pump cycle. Considering a mass exchange chamber of unit volume, the net mass of fluid pumped into the evaporator by one pump cycle is equal to the change in the mass within the mass exchange chamber during the period that valve CV2 is open, i.e. $\rho_3 - \rho_1$. This mass leaves the pump's evaporator as saturated liquid with specific enthalpy $h_{l,ev}$. During the period that valve CV2 is open, the mass flow of saturated vapour from the evaporator into the mass exchange chamber is $\rho_4 - \rho_3$ during process 3 → 4, and $\rho_{v,ev}$ during process 4 → 1. The mass of liquid received from the mass exchange chamber during process 4→1 is ρ_4, with specific enthalpy h_4. The heat input to the pump per unit of mass pumped is therefore

$$q_{in,pump} = \frac{h_{l,ev}(\rho_3 - \rho_1) + h_{v,ev}(\rho_4 - \rho_3) + h_{v,ev}\rho_{v,ev} - h_4\rho_4}{(\rho_3 - \rho_1)}. \tag{10}$$

The four terms in the numerator of Eq. 10 correspond to the discharge of saturated liquid from the evaporator, the vapour released during process 3 → 4, the vapour released during process 4 → 1, and the liquid received during process 4 → 1. The specific heat output from the pump's condenser can be found by considering energy conservation across the whole pump analysis system, and noting that the enthalpy gain through the pump is $h_{l,ev} - h_{l,c}$.

$$q_{out,pump} = q_{in,pump} - (h_{l,ev} - h_{l,c}). \tag{11}$$

Noting that heat addition in the evaporator is at temperature T_{ev} the exergy input to the TFE pump is

$$x_{q,in,pump} = \left(1 - \frac{T_0}{T_{ev}}\right) q_{in,pump}. \tag{12}$$

2.4 Advanced TFE pump configurations

In addition to the basic TFE pump depicted in Fig. **1**(denoted *TFE-basic-1*), two enhancements are proposed and analysed. First, the impact of introducing an 'economiser' heat exchanger in between the mass exchanger and the evaporator is considered (referred to as the *TFE-econ-1* configuration). The economiser heats sub-cooled liquid from the mass exchange chamber to the saturated liquid state before it passes into the pump's evaporator. Second, a two-stage version of the basic TFE pump is considered, referred to as the *TFE-basic-2* configuration, which includes an intermediate evaporator and a second mass exchange chamber. Last, Fig. 3 shows the two-stage TFE pump also including an economiser in the high-pressure stage, referred to as the *TFE-econ-2* configuration.

The heat inputs to the economiser in the *TFE-econ-1* configuration can be evaluated by considering conservation of energy in the economiser. For a mass exchange chamber with unit volume, the economiser receives mass ρ_4 of liquid with specific enthalpy h_4 during process 4 → 1, and delivers the same mass to the evaporator as saturated liquid with enthalpy $h_{l,ev}$. Therefore the heat input to the economiser per unit of mass pumped is

$$q_{in,econ.} = \frac{(h_{l,ev} - h_4)\rho_4}{(\rho_3 - \rho_1)}. \tag{13}$$

The *TFE-econ-1* pump evaporator now receives mass ρ_4 of saturated liquid from the economiser and supplies $\rho_4 - \rho_3$ of dry-saturated vapour to the mass exchange chamber during process 3 → 4, and $\rho_{v,ev}$ of vapour during process 4 → 1. The energy balance for the pump evaporator for one cycle gives,

$$q_{in,evap.} = (h_{v,ev} - h_{l,ev}) \frac{(\rho_{v,ev} + \rho_4 - \rho_3)}{(\rho_3 - \rho_1)}. \tag{14}$$

Recalling that $\rho_1 = \rho_{v,ev}$, it is evident that the total heat input for the *TFE-econ-1* pump found by summing Eqs. 13 and 14 is equal to the heat input for the *TFE-basic-1* pump given by Eq. 10. Therefore the heat output for the *TFE-econ-1* pump is also given by Eq. 11. The temperature of heat addition in the economiser is lower than the evaporation temperature however, so the specific exergy input to the *TFE-econ-1* pump is somewhat lower, given by,

$$x_{q,in,pump} = \frac{(\psi_{l,ev} - \psi_4)\rho_4}{(\rho_3 - \rho_1)} + \left(1 - \frac{T_0}{T_{ev}}\right) q_{in,evap}. \tag{15}$$

Assuming that the intermediate evaporator pressure is not subject to cyclic variations, the high- and low-pressure stages of the two-stage TFE pumps can be analysed independently using Eqs. 10-15, taking care to substitute the intermediate evaporator conditions for the evaporator and condenser

conditions when analysing the low-pressure and high-pressure stages respectively. The heat output from the high-pressure stage combined with any net heat input to the intermediate evaporator contribute the heat input to the low-pressure stage. Assuming cyclic-steady-state operation, the intermediate pressure level can be determined iteratively for any specified heat input to the intermediate evaporator – the Matlab® non-linear equation solver function *fzero* has been used for this purpose in this study [21,22].

3. Results and Discussion

Feed pump performance has been evaluated by considering an un-recuperated sub-critical ORC operating with pentane. Representative values of superheat $\Delta T_{super} = 4°\mathrm{C}$ and expander isentropic efficiency $\eta_{s,exp} = 70\%$ [2] are kept fixed throughout the analysis. The mechanical feed pump is modelled with an isentropic efficiency $\eta_{s,pump}$= 50%, representing a state-of-the-art pump efficiency for kW-scale ORC applications [2], and alternatively with an ideal isentropic efficiency $\eta_{s,pump}$= 100%, in order to illustrate the impact of having no thermodynamic irreversibility in the mechanical pump. Hereafter the cycles with mechanical feed pumps with 50% and 100% isentropic efficiency are denoted *real-mechanical* and *ideal-mechanical* pumps respectively. Qualitatively similar results to those presented below have been obtained for a range of superheat values $0°\mathrm{C} < \Delta T_{super} < 20°\mathrm{C}$ and for a wide range of expander isentropic efficiencies $30\% < \eta_{s,exp} < 90\%$. Cycle efficiencies are also shown for four additional working fluids (R1234yf, R134a, R245fa, and toluene) in Section 3.3, confirming that the conclusions drawn have a wide domain of applicability.

Heat is supplied to the ORC boiler and feed pump (where applicable) by an exhaust stream that is modelled as an isobaric flow of a perfect gas with constant pressure specific heat capacity $c_{p,ex} = 1.05\ kJ/kg/K$. The pinch point temperature difference in the boiler is fixed equal to $\Delta T_{pinch} = 10°\mathrm{C}$. The exhaust stream temperature is varied and the ORC evaporator pressure is adjusted in order to maximise the First Law overall efficiency.

3.1 Pump efficiency

Figure 4 compares the First Law pump efficiency $\eta_{I,pump}$ of the TFE and mechanical pump configurations. Both single-stage and both two-stage TFE pumps require the same total heat inputs and therefore display the same First Law efficiencies. Their First Law efficiencies are less than 100% because a portion of the heat added is rejected from the pump. The mechanism by which the TFE pumps reject heat is by allowing relatively hot vapour to flow upward through CV1 and CV2 and into the condenser, counter to the downward flow of relatively cold liquid through NRV1 and NRV2. The two-stage pumps have greater First Law pump efficiencies, compared to the single-stage pumps, because a smaller proportion of hot vapour passes upstream due to the smaller pressure difference in each stage.

Figure 4 indicates that $\eta_{I,pump}$ for the basic TFE pump is similar to the efficiency of a mechanical pump in an ORC with realistic component efficiencies. The reduction in efficiency of the TFE pumps at higher evaporation temperatures is partly due to the reduction of the saturated liquid-vapour density ratio in the evaporator at higher temperature, leading to a greater mass of vapour passing upward through the pump, relative to the mass of liquid pumped.

The two-stage pump results in Fig. 4 are obtained by specifying zero net heat input in the intermediate evaporator. Figure 5 shows that zero net heat input to the intermediate evaporator gives the maximum First Law pump efficiency. This condition also maximises the Second Law pump efficiency for the two-stage TFE-econ-2 pump. Therefore this optimal condition is adopted for all subsequent calculations involving two-stage pump configurations.

The Second Law pump efficiencies are shown in Fig. 6. The ideal mechanical feed pump has a Second Law pump efficiency of 100% because the pump and the economiser are both assumed to be internally reversible. At low evaporator temperatures the TFE-econ-1 and TFE-econ-2 pumps have similar Second-Law efficiencies to the real mechanical pump, however their efficiencies decline at higher evaporator temperature. The TFE-basic-1 and TFE-basic-2 have significantly higher exergy input and lower Second Law efficiencies, compared to the pumps with economisers, because they accept heat exclusively at the high-temperature T_{ev}. The basic TFE pumps destroy exergy through thermal dissipation as relatively cold liquid from the mass-exchange chamber flows directly into the hot evaporator drum. The benefit of the economiser is to enable heat addition at lower temperature, and to heat the sub-cooled liquid from the mass exchange chamber to the evaporation temperature in an internally-reversible process.

Additional sources of thermodynamic irreversibility are the viscous dissipation due to the pressure difference when valves CV1 and CV2 first open, and the ensuing thermal mixing between hotter vapour and colder liquid. The overall quantity of exergy destruction due to thermal mixing and viscous dissipation is reduced by introducing additional pumping stages because the pressure and temperature changes across each stage are smaller, as illustrated in Fig. 5 by the improved Second Law pump efficiency of the two-stage TFE pumps compared to the corresponding single-stage TFE pumps.

3.2 Cycle efficiency

The effect of pump type on cycle efficiency is shown in Fig. 7. The differences between pump performance become increasingly significant as the evaporator temperature approaches the critical temperature for two reasons. First, the back work ratio for the mechanical pumps increases with evaporator temperature, as shown in Fig. 8, making the cycle efficiency more sensitive to the irreversibilities in the expander and the feed pump. Second, the proportion of mass that travels upstream as hot vapour in the TFE pumps increases due to the relatively smaller difference between the liquid and vapour densities, particularly in the single-stage configurations. Remarkably, the First Law cycle efficiency for the two-stage TFE pump is greater than for the ideal mechanical feed pump. Despite having 100% isentropic efficiency, the ideal mechanical pump consumes power from the ORC with a cycle efficiency less than 16% - indicating that more than 84% of the heat consumed in order to power the pump is wasted. In contrast, the TFE pumps run directly on heat and Fig. 5 indicates that at optimal conditions the two-stage TFE pumps waste less than 1% of the heat provided.

3.3 Pump performance with alternative working fluids

The cycle analysis has been repeated for four additional organic working fluids: R1234yf, R134a, R245fa and toluene. The back work ratios for simple ORCs using these working fluids are presented in Fig. 8, confirming the observation by Quoilin et al. [2] that the back work ratio is greater for the fluids with lower critical temperatures (R1234yf, R134a, R245fa, pentane, toluene, water in order of increasing critical temperature).

The First Law cycle efficiencies for R1234yf, R134a, R245fa and toluene are presented in Fig. 9, and these may be compared with the corresponding results for pentane in Fig. 7. The efficiency predictions show that the thermal fluid exchange pump configurations provide similar advantages for each of these working fluids, with the two-stage configurations providing the best efficiency in every case. It is also found that the thermal fluid exchange pump provides the greatest relative increase in cycle efficiency for working fluids with lower critical temperatures: For a high-temperature ORC using toluene, the two-stage TFE pump offers a relative increase in cycle efficiency

of around 5% compared to a real mechanical pump whereas, for a low-temperature ORC using R1234yf or R134a, the two-stage TFE pump offers a relative increase of the cycle's efficiency of 20-30%.

3.4 Overall efficiency

The overall efficiency depends on the boiler efficiency as well as the cycle efficiency. The TFE pump type affects the boiler efficiency because it sets the location of the *pinch point* and therefore how much heat can be extracted from the exhaust. The TFE-basic-1 and TFE-basic2 pump configurations require all of the heat input at temperature T_{ev}, leading to a high exhaust exit temperature (as indicated in Fig. 2) and a relatively low boiler efficiency. The boiler efficiencies are shown in Fig. 7 as a function of the exhaust inlet temperature. Introducing an economiser into the TFE pumps reduces the exhaust exit temperature by transferring heat to sub-cooled liquid in the economiser. The boiler efficiency for the *TFE-econ-1* pump is very close values for the mechanical pumps because the working fluid enters the economisers at similarly cold conditions. In the two-stage TFE -economiser pump the exhaust temperature must be above the intermediate evaporator temperature, leading to a reduced boiler efficiency.

The overall efficiencies for the different feed pump configurations considered are shown in Fig. 11. The TFE pumps without economisers give relatively low overall efficiencies, due to their low boiler efficiencies. For exhaust inlet temperatures below 240°C, the pinch-point occurs at the evaporator and the TFE pumps with economisers give similar overall efficiencies to the real-mechanical pump. For higher exhaust temperatures, the pinch point occurs at the exhaust exit, and the overall efficiency for the *TFE-econ-1* and *TFE-econ2* pumps are both approximately 1% lower than for the real-mechanical pump, but for different reasons: the single-stage TFE-economiser efficiency decreases due to deteriorating cycle efficiency, whereas the two-stage TFE-economiser efficiency falls due to poor boiler efficiency.

The TFE-econ-2 configuration is particularly attractive because it gives *both* superior First Law cycle efficiency (15.3% compared to 14% for a high-efficiency mechanical pump operating with iso-pentane at $T_{ev} = 190°C$) and it also yields First Law overall efficiencies close to those for the mechanical pumps considered.

In many applications the minimum exhaust temperature is constrained by practical considerations. For example the small-scale gas turbine bottoming cycle application studied by Clemente et al. [23] required a minimum exhaust exit temperature of 70°C. This practical limitation imposes a maximum boiler efficiency of 80% at $T_{ev} = 250°C$, removing the advantage of the mechanical pumps so that the TFE-econ-2 pump, which has the highest cycle efficiency, also offers the highest overall efficiency.

4. Conclusions

Thermodynamic analysis of the recently proposed thermal fluid exchange pump has been presented and compared with the performance of mechanical feed pumps in the context of Organic Rankine Cycles. Two developments of the basic TFE pump have been proposed and analysed. First, a two-stage version of the basic TFE pump displays an improved First Law cycle efficiency. The First Law cycle efficiency exceeds the efficiency that could be obtained with an ideal mechanical pump. The two-stage configuration outperforms the one-stage configuration because the lower pressure difference across each stage leads to less hot vapour passing backwards through the pump, reducing the heat input required. It has been shown that the First Law cycle efficiency of the two-stage TFE pump is maximised when there is no net heat input to the intermediate evaporator. Practically, this

condition is also the simplest to implement since there is no requirement for a heat exchanger in the intermediate evaporator. Second, inserting an economiser within the TFE pump improves the boiler efficiency for the ORC. The resulting boiler efficiencies are practically the same as for mechanically-pumped ORCs. Adding the economiser to the two-stage TFE pump leads to an ORC whose cycle efficiency exceeds that of an ORC with an ideal mechanical pump *and* that achieves overall efficiencies practically the same as for the mechanical pumps considered. The results of this study indicate that the TFE pump concept has potential to compete with traditional mechanical ORC feed pumps in terms of efficiency – offering a substantial efficiency gain for ORC applications operating below 100°C.

Acknowledgement

The author acknowledges gratefully funding received from EPSRC grant EP/I004564/1 during this work.

References

[1] Chen, H., Yogi Goswami, D., Stefanakos, E.K., "A review of thermodynamic cycles for the conversion of low-grade heat" Renewable and Sustainable Energy Reviews 14 (2010) 3059-3067.
[2] Quoilin, S., van den Broek, M., Declaye, S., Dewallef, P., Lemort, V., "Techno-economic survey of Organic Rankine Cycle (ORC) systems" Renewable and Sustainable Energy Reviews 22 (2013) 168–186.
[3] Quoilin S., Lemort V., Lebrun J. Experimental study and modelling of an Organic Rankine Cycle using scroll expander. Applied Energy 2010; 87(4):1260–8.
[4] Quoilin S., Sustainable energy conversion through the use of Organic Rankine Cycles for waste heat recovery and solar applications. Phd thesis, University of Liège, Belgium, 2011.
[5] Bala E.J., O'Callaghan P.W., Probert S.D., Influence of organic working fluids on the performance of a positive-displacement pump with sliding vanes. Applied Energy 1985; 20:153–159.
[6] Trapp, C., Colonna, P., "Efficiency Improvement in Precombustion CO_2 Removal Units with a Waste-Heat Recovery ORC Power Plant", Journal of Engineering for Gas Turbines and Power, 135 (2013) 042311:1–12.
[7] Savery, T., "The Miner's Friend; or An Engine to Raise Water by Fire" republished by McCormick, London (1829).
[8] Riley, J.C. "The Pulsometer Steam Pump" Technology Quarterly and Proceedings of the Society of Arts. 8 14 (1901) 243–254.
[9] Smith, T.C.B. "Non Inertive-Feedback Thermofluidic Engine", PhD Thesis, University of Cambridge (2005).
[10] Markides, C.N. Osuolale, A. Solanki, R. Stan, G.V., Nonlinear heat transfer processes in a two-phase thermofluidic oscillator. Applied Energy 104 (2013) 958–977.
[11] Yamada, N., Watanabe, M., Hoshi, A., Experiment on pumpless Rankine-type cycle with scroll expander, Energy 49(2013)137–145.
[12] Vaisman, I.B., Sangiovanni, J.J. Taras, M.F., US Patent Application No. PCT/US07/12567, June (2010).
[13] Çengel Y.A., Boles, M.A. "Thermodynamics, An Engineering Approach" 7th Edition, McGraw Hill, New York, 2011.
[14] Horlock J.B. "Combined Power Plants Including Combined Cycle Gas Turbine (CCGT) Plants" Pergamon Press, Oxford, 1994.
[15] Span, R. and Wagner, W. "Equations of State for Technical Applications. II. Results for Nonpolar Fluids," Int. J. Thermophys., 24(1):41-109, 2003.

[16] Richter, M., McLinden, M.O., and Lemmon, E.W. "Thermodynamic Properties of 2,3,3,3-Tetrafluoroprop-1-ene (R1234yf): Vapor Pressure and p-rho-T Measurements and an Equation of State," J. Chem. Eng. Data, 56(7):3254-3264, 2011.

[17] Tillner-Roth, R. and Baehr, H.D.,"An international standard formulation of the thermodynamic properties of 1,1,1,2-tetrafluoroethane (HFC-134a) for temperatures from 170 K to 455 K at pressures up to 70 MPa," J. Phys. Chem. Ref. Data, 23:657-729, 1994.

[18] Lemmon, E.W. and Span, R., "Short Fundamental Equations of State for 20 Industrial Fluids," J. Chem. Eng. Data, 51:785-850, 2006.

[19] Wagner, W. and Pruss, A., "The IAPWS Formulation 1995 for the Thermodynamic Properties of Ordinary Water Substance for General and Scientific Use," J. Phys. Chem. Ref. Data, 31(2):387-535, 2002.

[20] Lemmon, E.W., Huber, M.L., McLinden, M.O. NIST Standard Reference Database 23: Reference Fluid Thermodynamic and Transport Properties-REFPROP, Version 9.1, National Institute of Standards and Technology, Standard Reference Data Program, Gaithersburg, 2013.

[21] Brent, R.P., “Algorithms for Minimization Without Derivatives”, Prentice-Hall, 1973.

[22] Forsythe, G. E., M. A. Malcolm, and C. B. Moler, “Computer Methods for Mathematical Computations”, Prentice-Hall, 1977.

[23] Clemente, S., Micheil, D., Reini, M., Taccani, R., “Bottoming organic Rankine cycle for a small scale gas turbine: A comparison of different solutions” Applied Energy 106 (2013) 355-364.

Appendix: Flow rate estimation

In this section, estimates are derived for key operating parameters of the Thermal Fluid Exchange pump. In combination with the thermodynamic efficiencies presented in the paper, these estimates may be used to develop a preliminary specification for components in Thermal Fluid Exchange pumps for Organic Rankine Cycle applications. The main parameters of interest are the cycle duration and the time-averaged mass flow rate through the pump.

The pressure-difference driving the flow through the control valves during processes 1→2 and 3→4 are of the order of magnitude of the difference between the evaporator and condenser saturation pressures, and these pressure differences are expected to be much greater than the hydrostatic pressure differences across the control and non-return valves during processes 2→3 and 4→1. Therefore, assuming that the cycle time is dominated by the time taken for buoyancy-driven flow of liquid through the non-return valves, the total cycle time may be estimated by the time taken to fill and then to drain the liquid in the mass exchange chamber:

$$\tau_{cycle} \approx \tau_{23} + \tau_{41}. \tag{A.1}$$

For the purpose of estimating τ_{23} and τ_{41}, it is also assumed that the flow resistance of the control valves is much less than the flow resistance of the corresponding non-return valves, so that the pressure difference acting across the non-return valves can be calculated from the head of liquid above the valve, and it is assumed that the flow velocities are sufficiently small during the buoyancy-driven processes that inertia of the fluid is negligible throughout the system. Modelling the flow through the first non-return valve with a constant discharge coefficient $C_{d,1}$ and valve area A_1, the rate of change of the mass of liquid in the mass exchange chamber, m_l, due to flow through NRV1 is estimated to be,

$$\left(\frac{dm_l}{dt}\right)_{23} = +C_{d,1}A_1\sqrt{2\rho_{l,c}\Delta p_1}, \tag{A.2}$$

where the pressure difference Δp_1 across NRV1 depends on the vertical distance L_1 between NRV1 and the level of the liquid-vapour interface in the condenser. Estimating the liquid-vapour density difference to be $\rho_{l,c} - \rho_{v,c}$,

$$\Delta p_1 = \left(\rho_{l,c} - \rho_{v,c}\right)gL_1. \tag{A.3}$$

g ≈9.8m/s^2 is the acceleration due to gravity. The non-return valve and the length L_1 should be specified so that the differential pressure Δp_1 is sufficient to overcome fully the retaining spring in the non-return valve.

The filling time τ_{23} is obtained by integrating Eq. A.2 until the chamber volume V is full of saturated liquid with density $\rho_{l,c}$,

$$\int_0^{\tau_{23}} dt = \frac{1}{C_{d,1}A_1\sqrt{2\rho_{l,c}\left(\rho_{l,c} - \rho_{v,c}\right)gL_1}}.\int_0^{V.\rho_{l,c}} dm_l, \tag{A.4}$$

leading to

$$\tau_{23} = \frac{\rho_{l,c} V}{C_{d,1} A_1 \sqrt{2\rho_{l,c}(\rho_{l,c} - \rho_{v,c}) g L_1}}. \tag{A.5}$$

Assuming a constant flow rate through the expander, the expected peak-to-peak variation in the volume of liquid within the condenser during the cycle is estimated by considering that liquid drains from the condenser during a time interval τ_{23} whereas it refills over the whole cycle period τ_t. Therefore the fluctuation in the liquid volume will be approximately $(1 - \tau_{23}/\tau_t)V$, assuming constant temperature and saturated conditions in the condenser. The capacity for liquid in the condenser should be greater than $(1 - \tau_{23}/\tau_t)V$ to avoid it running dry when filling the mass exchange chamber.

The rate of change of the mass of liquid in the mass exchange chamber due to the flow of liquid through NRV2 is estimated to be

$$\left(\frac{dm_l}{dt}\right)_{41} = -C_{d,2} A_2 \sqrt{2\rho_{l,c} \Delta p_2}, \tag{A.6}$$

where $C_{d,2}$ is a constant discharge coefficient and A_2 is the cross-sectional area of NRV2. The pressure drop across NRV2 is given by

$$\Delta p_2 = (\rho_{l,c} - \rho_{v,c}) g (L_2 + m L_\Delta / \rho_{l,c} V), \tag{A.7}$$

where the height between the non-return valve and the liquid surface in the mass exchange chamber is given by the sum of the depth of liquid within the mass exchange chamber and the height of the pipe connecting mass exchange chamber to the second non-return valve, L_2. The length L_2 should be specified so that the liquid within the pipe provides sufficient head to fully open NRV2 even when the mass of liquid in the mass exchange chamber m_l falls to zero. For a prismatic mass exchange chamber, the depth of liquid within the chamber may be expressed as $m_l L_\Delta / \rho_{l,c} V$, where L_Δ is the height of the chamber. The emptying time τ_{41} is obtained by integrating the mass flow rate during process 4→1.

$$\int_0^{\tau_{41}} dt = -\frac{1}{C_{d,2} A_2 \sqrt{2\rho_l (\rho_{l,c} - \rho_{v,ev}) g L_\Delta}} . \int_{\rho_{l,c} V}^{0} \frac{1}{\sqrt{\left(\frac{L_2}{L_\Delta} + \frac{m_l}{\rho_{l,c} V}\right)}} dm_l \tag{A.8}$$

giving,

$$\tau_{41} = \frac{2\rho_{l,c} V}{C_{d,2} A_2 \sqrt{2\rho_{l,c}(\rho_{l,c} - \rho_{v,ev}) g L_\Delta}} . \left[\sqrt{1 + \frac{L_2}{L_\Delta}} - \sqrt{\frac{L_2}{L_\Delta}}\right]. \tag{A.9}$$

Assuming a constant flow rate through the expander, the expected peak-to-peak variation in the volume of liquid within the expander during the cycle is estimated by considering that liquid enters the evaporator during a time interval τ_{41}, whereas the evaporator supplies vapour to the expander

over the whole cycle period τ_t. Therefore the fluctuation in the liquid volume will be approximately $(1 - \tau_{41}/\tau_t)V$, assuming constant saturated conditions.

The total mass flow rate during one cycle is $m_t \approx \left(\rho_{l,c} - \rho_{v,ev}\right)V$, and therefore the cycle-averaged mass flow rate is estimated to be,

$$\dot{m}_t \approx \frac{\left(\rho_{l,c} - \rho_{v,ev}\right)V}{\tau_{23} + \tau_{41}}. \tag{A.10}$$

From the equations above, it is apparent that the cycle-averaged mass flow rate can be enhanced first by reducing flow resistances (i.e. by increasing valve areas and discharge coefficients, or placing multiple valves in parallel), and second, by increasing the pressure differences across the non-return valves (i.e. by increasing L_1, L_2 and L_Δ). According to this estimate, the volume of the mass-exchange chamber is proportional to the cycle duration but, since it is also proportional to the mass pumped per cycle, it does not have a strong influence on the cycle-averaged mass flow rate achieved by the pump. Therefore the volume of the mass exchange chamber may be specified to optimise other objectives: On one hand, a larger mass exchange chamber volume will lead to fewer pump cycles for a given flow and therefore fewer actuations and less wear of the control valves. A large mass exchanger volume is therefore attractive in order to extend the service life of the control valves. On the other hand, a larger mass exchange volume leads to larger fluctuations of the liquid volume in the condenser and evaporator, requiring larger and more costly condenser, evaporator and mass exchange components, as well as a greater charge of working fluid. The most economic choice of mass exchange chamber volume therefore depends on the costs of manufacturing, installing and servicing the respective components, and the performance estimates derived above provide a basis for determining the most economic choice of components for a given application.

Table 1: The four states and processes in the TFE pumping cycle

State 1	The minimum liquid level in the mass-exchange chamber, CV2 is open, $p = p_{ev}$
Process 1 → 2	CV2 is closed and then CV1 is opened. Vapour flows from the mass-exchange chamber into the condenser until their pressures reach equilibrium.
State 2	CV1 is open, $p = p_c$
Process 2 → 3	CV1 remains open. Buoyancy drives a flow of liquid from the condenser into the mass-exchange chamber through NRV1.
State 3	The maximum liquid level in the mass-exchange chamber, CV1 is open, $p = p_c$
Process 3 → 4	CV1 is closed and then CV2 opened. Vapour flows from the evaporator into the mass-exchange chamber until the pressures reach equilibrium.
State 4	CV2 is open, $p = p_{ev}$.
Process 4 → 1	CV2 remains open. Buoyancy drives a flow of liquid from the mass-exchange chamber into the evaporator through NRV2.

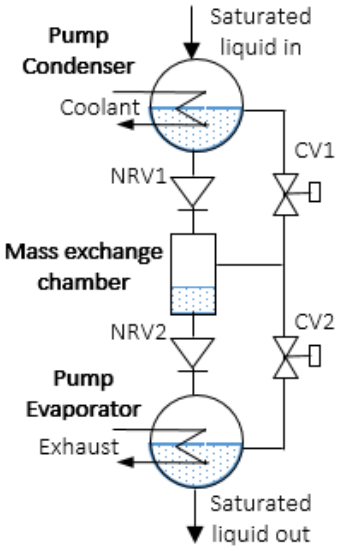

Figure 1: The basic TFE pump configuration.

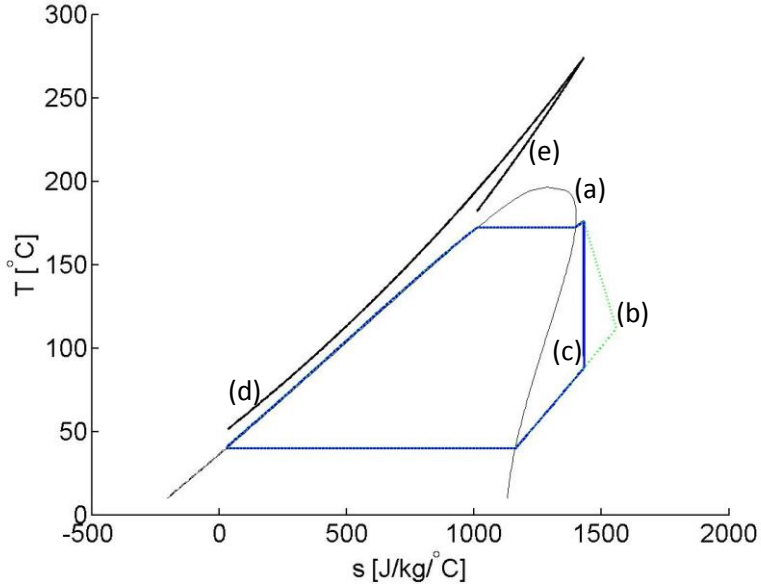

Figure 2: Temperature-entropy plot showing: (a) the saturation curve for pentane; (b) an ORC; (c) the basic TFE pumping cycle; and the flow of exhaust gas through the boiler in in the case of a mechanical pump (d) and the basic TFE pump (e). The exhaust entropy is rescaled to match the range of the working fluid entropy in the boiler.

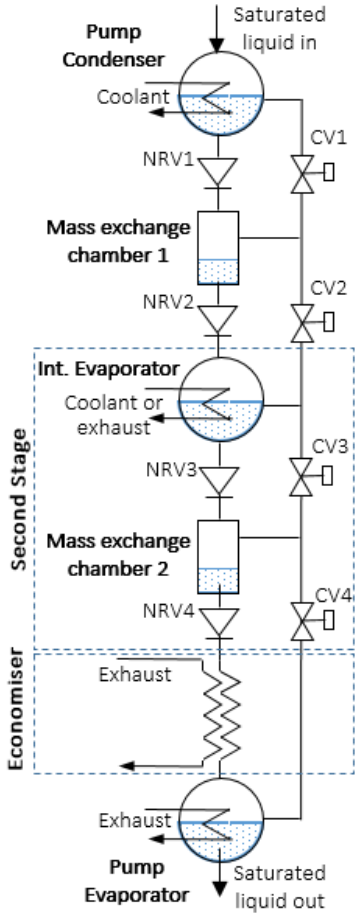

Figure 3. Configuration of the *TFE-econ-2* pump, consisting of a two-stage TFE pump with an economiser in the high pressure stage.

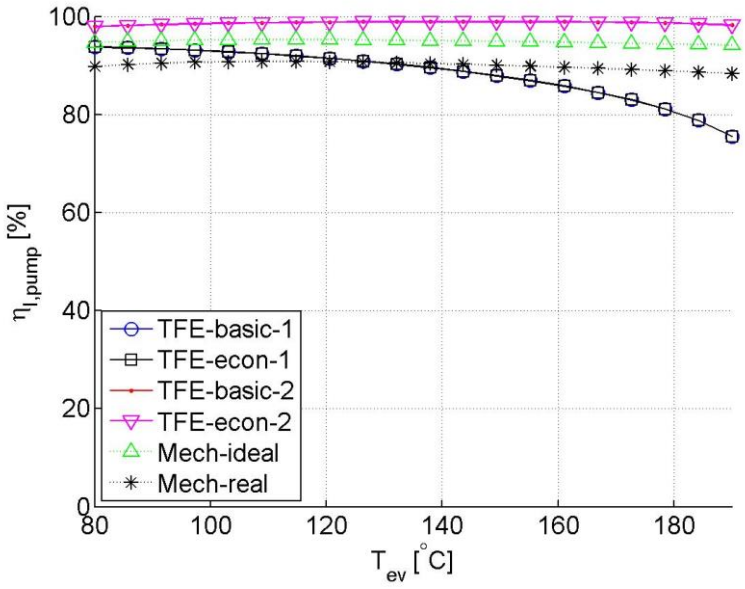

Figure 4. First Law pump efficiencies $\eta_{I,pump}$ versus evaporator temperature.

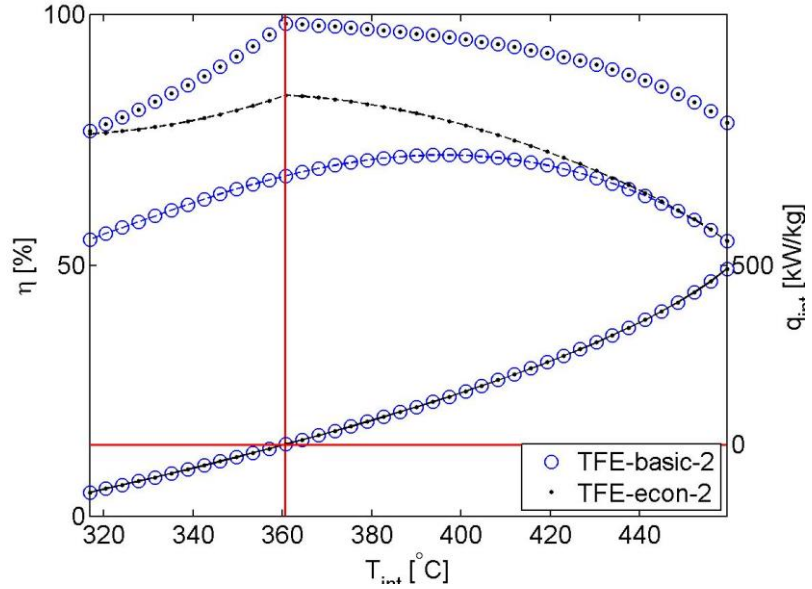

Figure 5. Pump efficiencies of two-stage TFE pumps versus the intermediate evaporator temperature with T_c=40°C and T_{ev}=190°C: (solid line) net specific heat input to the intermediate evaporator; (no line) First Law pump efficiency; (dashed line) Second Law pump efficiency.

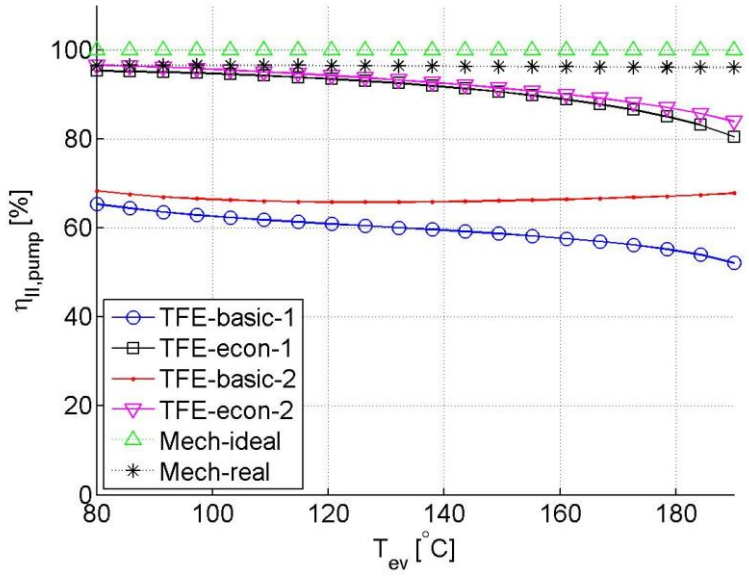

Figure 6. Second Law pump efficiencies $\boldsymbol{\eta_{II,pump}}$ versus evaporator temperature.

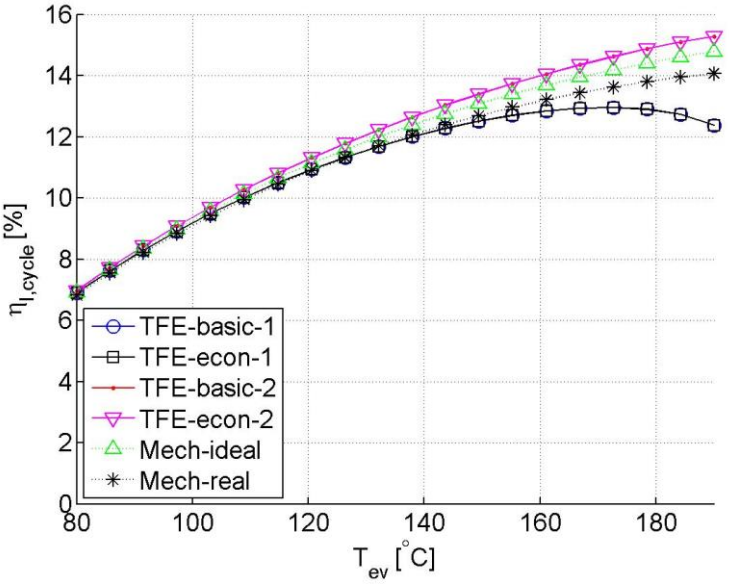

Figure 7. First Law cycle efficiencies $\eta_{I,cyc}$ versus evaporator temperature.

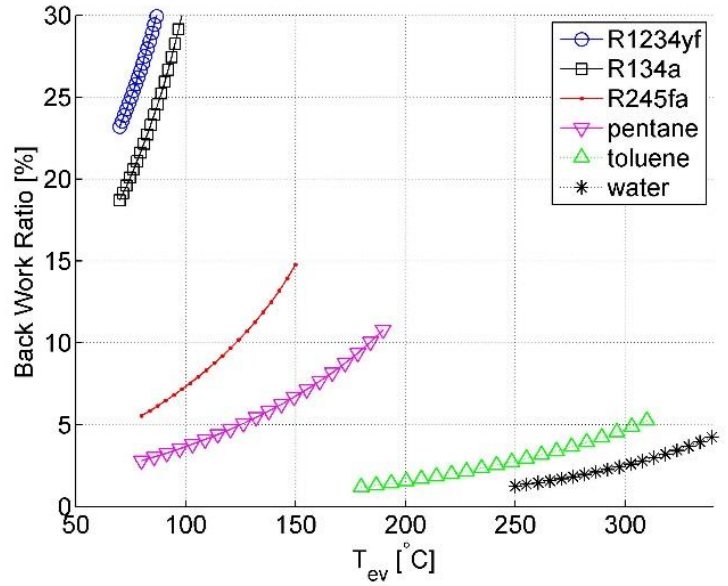

Figure 8. Back work ratio for simple Rankine cycles with R1234yf, R134a, R245fa, pentane, toluene and water working fluids.

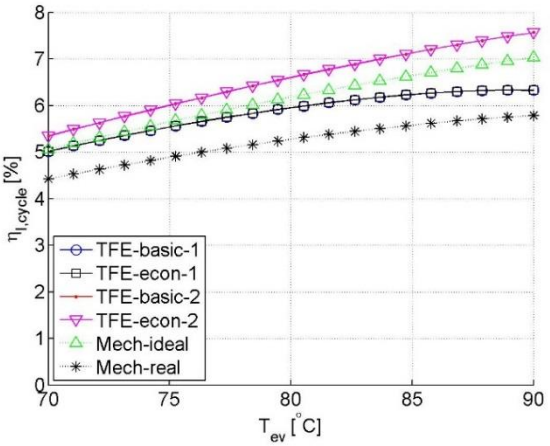
$\eta_{I,cycle}$ [%]
T_{ev} [°C]
TFE-basic-1
TFE-econ-1
TFE-basic-2
TFE-econ-2
Mech-ideal
Mech-real

(a)

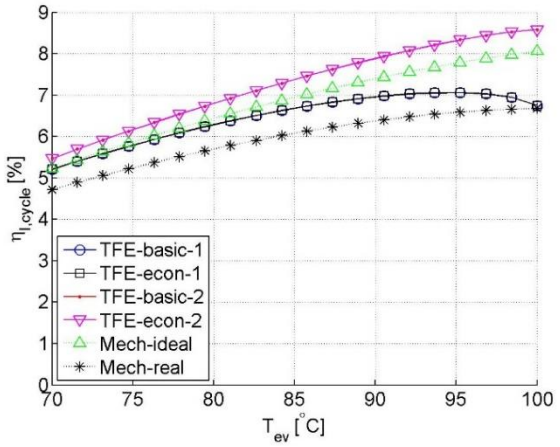
$\eta_{I,cycle}$ [%]
T_{ev} [°C]
TFE-basic-1
TFE-econ-1
TFE-basic-2
TFE-econ-2
Mech-ideal
Mech-real

(b)

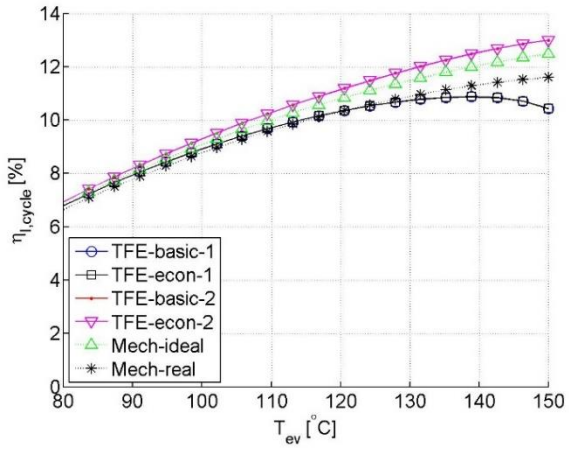
$\eta_{I,cycle}$ [%]
T_{ev} [°C]
TFE-basic-1
TFE-econ-1
TFE-basic-2
TFE-econ-2
Mech-ideal
Mech-real

(c)

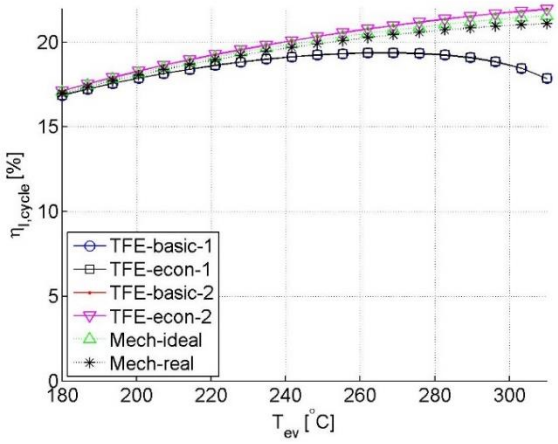

(d)

Figure 9. First Law cycle efficiencies for a range of evaporator temperatures and feed pump options, using (a) R1234yf, (b) R134a, (c) R245fa and (d) toluene.

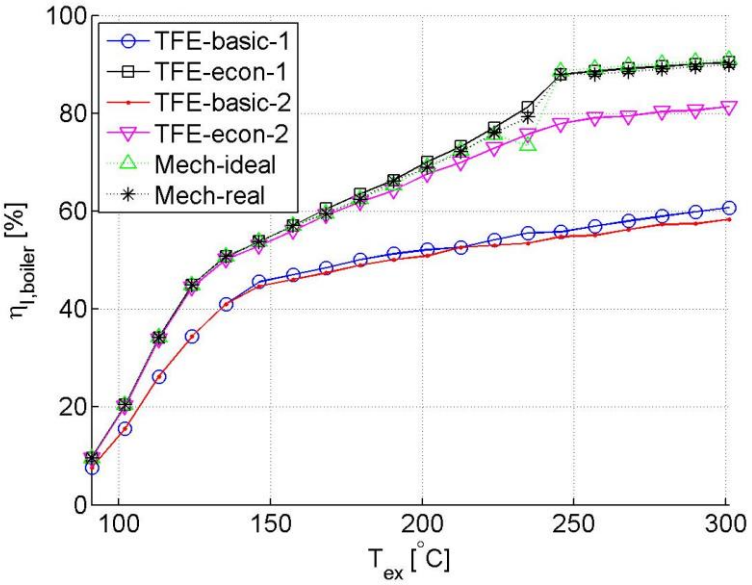

Figure 10. First Law boiler efficiencies $\eta_{I,b}$ versus exhaust temperature.

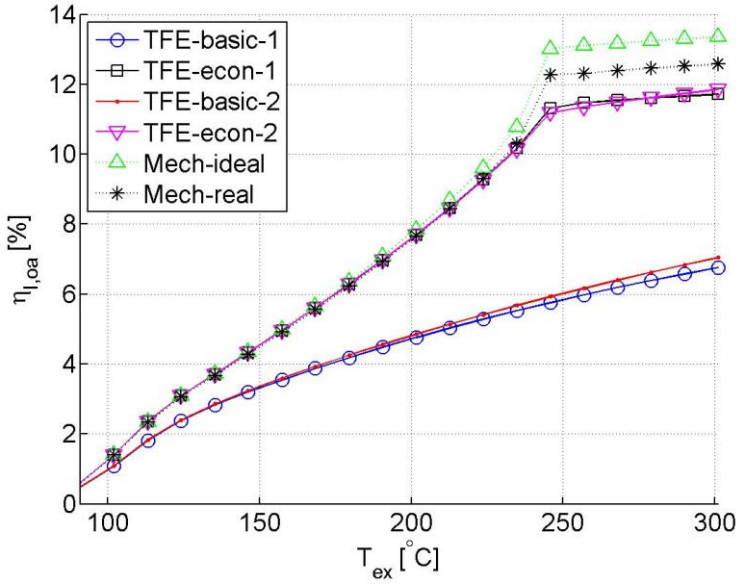

Figure 11. First Law overall efficiencies $\eta_{I,oa}$ versus exhaust temperature.